



UDC 542.943:546.831

<https://doi.org/10.17073/1997-308X-2023-3-30-37>

Research article

Научная статья



## High-temperature oxidation of $\text{ZrB}_2\text{-SiC-La}_2\text{O}_3$ ceramic material produced via spark plasma sintering

V. B. Kulmetyeva, V. E. Chuvashov, K. N. Lebedeva,  
S. E. Porozova<sup>✉</sup>, M. N. Kachenyuk

Perm National Research Polytechnic University  
29 Komsomolsky Prospekt, Perm 614000, Russia

sw.porozova@yandex.ru

**Abstract.** The study investigated the influence of  $\text{La}_2\text{O}_3$  addition on the oxidation properties of composite ceramics with a composition of 80 vol. %  $\text{ZrB}_2$  and 20 vol. % SiC. The source materials utilized in this study included zirconium diboride (DPTP Vega LLC, Russia), grade 63C silicon carbide (Volzhsky Abrasive Works JSC, Russia), and lanthanum hydroxide concentrate (Solikamsk Magnesium Plant JSC, Russia), with the following elemental content (wt. %): La – 54.2, Nd – 4.3, Pr – 2.8, and trace amounts of other elements (<0.1). The  $\text{La}_2\text{O}_3$  content in the charge varied between 0, 2 and 5 vol. %. The powders were mixed in a planetary mill with ethyl alcohol as the medium for 2 h, using a grinding media to powder ratio of 3:1. Consolidation of the powders was achieved through spark plasma sintering at 1700 °C, applying a pressing pressure of 30 MPa. The heating rate was 50 °C/min, and the isothermal holding time was 5 min. Oxidation was carried out in air at 1200 °C and the total oxidation time was 20 h. Oxidation experiments were conducted in air at 1200 °C, with a total oxidation time of 20 h. It was observed that the most significant weight gain occurred within the first 2–4 h of testing. Specimens containing 5 vol. %  $\text{La}_2\text{O}_3$  exhibited the smallest weight gain after 20 h of exposure. Regardless of the presence of  $\text{La}_2\text{O}_3$ , silicon carbide was found to be the first material to undergo oxidation. In specimens without  $\text{La}_2\text{O}_3$  addition, the oxidized layer mainly consisted of silicon monoxide and dioxide. In contrast, specimens with  $\text{La}_2\text{O}_3$  exhibited a predominantly oxidized layer composed of  $\text{ZrSiO}_4$  and  $\text{ZrO}_2$ . The study revealed that the introduction of  $\text{La}_2\text{O}_3$  intensified the formation of zircon, which subsequently slowed down the oxidation processes in the material.

**Keywords:** oxidation, spark plasma sintering, zirconium diboride, silicon carbide, lanthanum oxide, oxidized layer, energy dispersive analysis, elemental composition

**For citation:** Kulmetyeva V.B., Chuvashov V.E., Lebedeva K.N., Porozova S.E., Kachenyuk M.N. High-temperature oxidation of  $\text{ZrB}_2\text{-SiC-La}_2\text{O}_3$  ceramic material produced via spark plasma sintering. *Powder Metallurgy and Functional Coatings*. 2023;17(3):30–37. <https://doi.org/10.17073/1997-308X-2023-3-30-37>

## Особенности высокотемпературного окисления керамического материала $\text{ZrB}_2\text{-SiC-La}_2\text{O}_3$ , полученного искровым плазменным спеканием

В. Б. Кульметьева, В. Э. Чувашов, К. Н. Лебедева,  
С. Е. Порозова<sup>✉</sup>, М. Н. Каченюк

Пермский национальный исследовательский политехнический университет  
Россия, 614000, г. Пермь, Комсомольский пр-т, 29

sw.porozova@yandex.ru

**Аннотация.** Исследовано влияние добавки  $\text{La}_2\text{O}_3$  на окисление керамики состава, об. %: 80 $\text{ZrB}_2$ –20SiC. В качестве исходных материалов использовали диборид циркония (ООО ДПТП «Вега», Россия), карбид кремния марки 63С (ОАО «Волжский

абразивный завод», Россия) и концентрат гидроксида лантана (ОАО «Соликамский магниевый завод», Россия), содержание элементов в котором составляло, мас. %: La – 54,2, Nd – 4,3, Pr – 2,8, остальные – менее 0,1. Содержание  $La_2O_3$  в шихте варьировалось: 0, 2 и 5 об. %. Смешивание порошков проводили с использованием планетарной мельницы в течение 2 ч в этиловом спирте, соотношение мелющих тел и порошка составляло 3:1. Консолидацию порошков осуществляли методом искрового плазменного спекания при температуре 1700 °C и давлении прессования 30 МПа со скоростью нагрева 50 °C/мин и изотермической выдержкой 5 мин. Окисление проводили на воздухе при температуре 1200 °C, общее время окисления составило 20 ч. Наиболее интенсивное увеличение массы отмечено в течение первых 2–4 ч испытаний. По истечении 20 ч наименьшее увеличение массы наблюдалось у образцов с добавкой 5 об. %  $La_2O_3$ . Установлено, что вне зависимости от наличия  $La_2O_3$  карбид кремния первым подвергается окислению. В образцах без добавки  $La_2O_3$  окисленный слой состоит преимущественно из моно- и диоксида кремния, тогда как в образцах с  $La_2O_3$  большую часть окисленного слоя составляют  $ZrSiO_4$  и  $ZrO_2$ . Таким образом, установлено, что введение  $La_2O_3$  интенсифицирует процесс формирования циркона, что способствует замедлению процессов окисления.

**Ключевые слова:** окисление, искровое плазменное спекание, диборид циркония, карбид кремния, оксид лантана, окисленный слой, энергодисперсионный анализ, элементный состав

**Для цитирования:** Кульметьева В.Б., Чувашов В.Э., Лебедева К.Н., Порозова С.Е., Каченюк М.Н. Особенности высокотемпературного окисления керамического материала  $ZrB_2$ – $SiC$ – $La_2O_3$ , полученного искровым плазменным спеканием. *Известия вузов. Порошковая металлургия и функциональные покрытия*. 2023;17(3):30–37.

<https://doi.org/10.17073/1997-308X-2023-3-30-37>

## Introduction

To date, the primary concern lies in the development of materials capable of enduring extended periods in oxidizing environments at high temperatures [1–3]. In this regard, a noteworthy focus is on ultra-high-temperature ceramics (UHTC), which consist of a ceramic matrix and a protective structure that shields the surface from oxidation [1; 4; 5]. In order to produce such materials a deliberate selection of additive phases is conducted to facilitate the formation of surface structures that can withstand prolonged exposure to oxidizing environments at high temperatures. One prevalent example of UHTCs is composite materials based on zirconium or hafnium borides, which exhibit high thermal conductivity and thermal shock resistance [6].

Sintering zirconium and hafnium boride powders requires temperatures exceeding 1950 °C due to their strong covalent bonds and low self-diffusion coefficient [7; 8]. The sintering process is typically activated by incorporating sintering additives such as SiC,  $Si_3N_4$ ,  $La_2O_3$ ,  $LaB_6$  [9; 10], tantalum, titanium, zirconium, molybdenum silicides, etc. The optimum composition is considered to be the volumetric ratio of 80 %  $ZrB_2$  to 20 % SiC [11; 12]. At high temperatures, the oxidation of these ceramics leads to the formation of a protective multi-layer coating on the surface, consisting of  $ZrO_2$ – $SiO_2$  and borosilicate glass. This coating effectively seals cracks and pores on the UHTC surface, creating a gas-tight film that prevents oxygen diffusion into the material [13; 14].

Spark plasma sintering (SPS) is a relatively recent technique that enables the reduction of sintering temperature and time for certain materials when performed under vacuum or an argon atmosphere [15]. Despite some existing studies in this area, the phase composition, structure, and oxidation properties of boride-based com-

posite materials produced through this process have not been adequately investigated [15–17].

The objective of this study was to examine the impact of  $La_2O_3$  addition on the oxidation properties of composite ceramics with the following volumetric composition: 80 $ZrB_2$ –20SiC.

## Materials and Methods of Research

The source materials utilized in this study included:  
– zirconium diboride (DPTP Vega LLC., Russia);  
– lanthanum hydroxide concentrate (Solikamsk Magnesium Plant JSC, Russia), with the following elemental content (wt. %): La – 54,2, Nd – 4,3, Pr – 2,8 and trace amounts of other elements (<0,1);  
– grade 63C silicon carbide (Volzhsky Abrasive Works JSC, Russia).

The particle size distribution of the powders was determined using laser light diffraction with the Analysette 22 NanoTec plant (Fritsch GmbH, Germany). The  $ZrB_2$  powder exhibited a predominant particle size range of 0.5 to 12  $\mu m$ , with 97 % of particles measuring less than 11.1  $\mu m$ , and an average particle size of 4.52  $\mu m$ . The SiC powder demonstrated a bimodal particle size distribution, with an average particle size of 3.47  $\mu m$ . The  $La(OH)_3$  powder exhibited a wide particle size distribution, with an average particle size of 9.76  $\mu m$ .

In order to convert lanthanum hydroxide into oxide, the material was subjected to annealing at 600 °C for a duration of 1 h in an air atmosphere. The initial powders were mixed using a SAND planetary mill in ethyl alcohol. The grinding process lasted for 2 h at a speed of 160 rpm, a grinding media to powder ratio of 3:1. The mixtures contained lanthanum oxide in two different volumetric percentages: 0, 2 and 5.

The specimens were consolidated using spark plasma sintering (SPS) on the Dr. Synter SPS-1050b equipment

(SPS Syntex, Japan) at a temperature of 1700 °C. Heating was achieved by applying a pulsed direct current at a rate of 50 °C per min. The temperature was monitored using an optical pyrometer placed on the outer side of the graphite matrix. The material was loaded into the system just before the heating process began, while maintaining a constant load at a pressure of 30 MPa. The applied load was removed after the completion of the heating phase. To prevent any undesirable reactions between the sintered powder, matrix, and punches, graphite paper was employed. Additionally, graphite felt was wrapped around the mold to minimize heat losses. The specimens were subjected to an isothermal holding time of 5 min.

The apparent density and open porosity of sintered specimens were analyzed following the guidelines outlined in GOST 2409-2014.

For the oxidation study, the specimens were exposed to air in an electric furnace equipped with silicon carbide heaters. The crucibles containing the specimens were placed in the furnace, preheated to 1200 °C. After a specific duration, the specimens were removed, weighed to record their weight, and then returned to the furnace. The total duration of high-temperature oxidation was 20 h.

The phase composition of the specimens was examined using Raman spectroscopy on a multifunction spectrometer SENTERRA (Bruker, Germany), with a laser wavelength of 532 nm. The acquired data were processed using the OPUS 6.5 software.

Microscopic analysis of the specimens was conducted using an analytical auto emission scanning electron microscope VEGA3 (TESCAN, Czech Republic). In order to determine the elemental composition, an Inca X-Act detector (Oxford Instruments Analytical, Great Britain) was employed for energy-dispersive analysis of the elemental composition of the materials.

## Results and Discussion

The investigations were conducted on the materials containing 0, 2 and 5 vol. % of  $\text{La}_2\text{O}_3$ . No significant changes in the apparent density and open porosity of the specimens were observed after the SPS process. The open porosity values ranged from 3.5 to 5.5 % across all variations.

The specimens were subjected to oxidation in an air environment for a duration of 20 h. The time intervals for recording the specific weight gain of the specimens increased as the weight gain decreased. The results are presented in Figure 1. The most substantial weight gain occurred within the initial 2–4 h of testing.

Among the specimens, those with 5 vol. % of  $\text{La}_2\text{O}_3$  exhibited the lowest weight gain after the 20-hour exposure. It is worth noting that up to 9 h of exposure, the differences in specific weight gain were minimal. Only with further increases in oxidation time did the impact

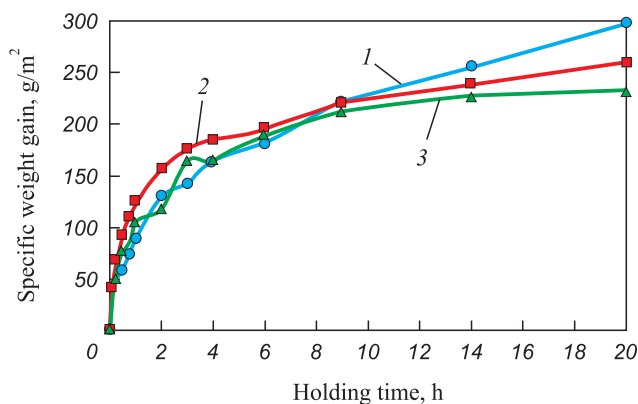


Fig. 1. Specific weight gain of  $\text{ZrB}_2$ -20 vol. % SiC ceramic specimens with different content of  $\text{La}_2\text{O}_3$  after oxidation for 20 h at 1200 °C  
 $\text{La}_2\text{O}_3$ , vol. %: 1 – 0, 2 – 2 and 3 – 5

Рис. 1. Удельный привес образцов керамики  $\text{ZrB}_2$ -20 об. % SiC с различным содержанием  $\text{La}_2\text{O}_3$  после окисления в течение 20 ч при  $t = 1200$  °C  
 $\text{La}_2\text{O}_3$ , об. %: 1 – 0, 2 – 2 и 3 – 5

of  $\text{La}_2\text{O}_3$  on the material's oxidation resistance become more pronounced.

It has been established that the resistance of  $\text{ZrB}_2$  composite materials to high-temperature oxidation is primarily influenced by the composition of the protective layer formed on the material's surface [18]. The fractures in the specimens were examined using scanning electron microscopy (SEM) along with energy dispersive analysis. SEM images and maps displaying the distribution of silicon, zirconium, and boron within the specimens were obtained (Figure 2: spectrum 1 represents the surface layer of the specimen; spectrum 2 corresponds to an internal structure displaying significant visual dissimilarity; spectrum 3 pertains to a deeper layer of the material).

In the specimen without the addition of  $\text{La}_2\text{O}_3$ , a continuous protective layer composed of silicon-containing phases is formed on its surface (spectrum 1 in Fig. 2). When  $\text{La}_2\text{O}_3$  is introduced, the silicon content on the specimen surface is also higher (spectrum 1) compared to the subsequent layers (spectra 2 and 3). However, the thickness of these layers is significantly reduced. Figure 3 presents a histogram depicting the calculated thickness of the oxidized layers, determined through analysis of the material's microstructure (as shown in Figure 2).

Table 1 displays the outcomes of the energy dispersive analysis, providing the elemental composition of the specimens following a 20-hour oxidation process. The first layer exhibits identical composition across all three cases. Notably, boron is not detected in the spectra, which is consistent with the challenges in accurately capturing elements from the second period of the periodic table using spectral methods [19].

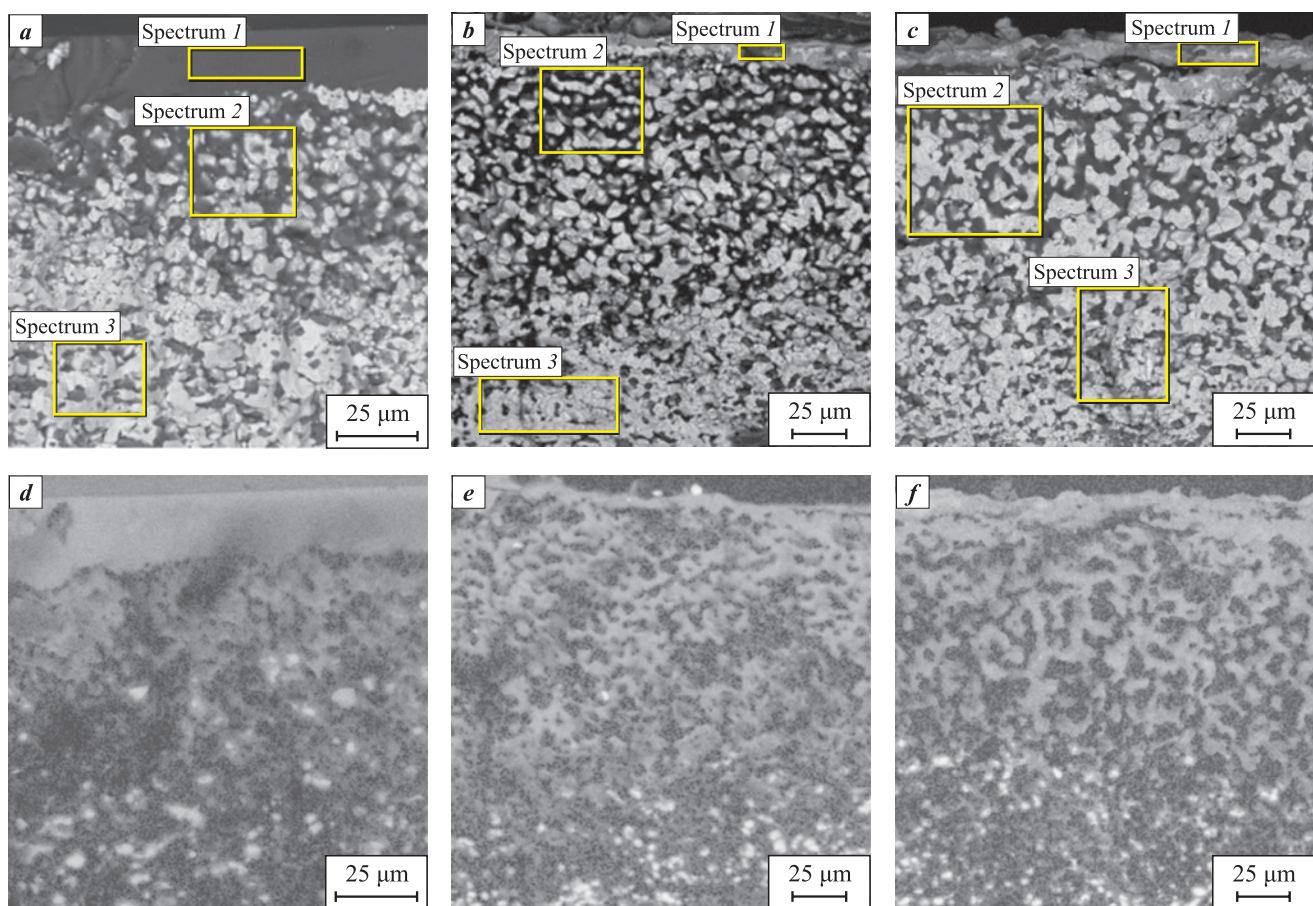


**Fig. 2.** SEM-images of fractures (a–c) and silicon distribution maps (d–f) after oxidation for 20 h of  $ZrB_2$ –20 vol. %  $SiC$  specimens  
Addition of  $La_2O_3$ , vol. %: 0 (a, d), 2 (b, e) and 5 (c, f)  
White and light gray colors on distribution maps – silicon-containing phases

**Рис. 2.** СЭМ-изображения изломов (а–с) и карты распределения кремния (д–ф) после окисления в течение 20 ч образцов состава  $ZrB_2$ –20 об. %  $SiC$   
Добавка  $La_2O_3$ , об. %: 0 (а, д), 2 (б, е) и 5 (с, ф)  
Белый и светло-серый цвета на картах распределения – кремнийсодержащие фазы

**Table 1. Outcomes of the energy dispersive analysis of the elemental composition of the specimens after oxidation for 20 h**

**Таблица 1. Результаты энергодисперсионного анализа элементного состава образцов после окисления в течение 20 ч**

Imaging place (see Figure 2)	Elemental composition (wt. %) with the addition of $La_2O_3$ , vol. %		
	0	2	5
Spectrum 1 Upper layer	O – 40.43 Si – 54.45 Zr – 2.90	O – 33.36 Si – 12.12 Zr – 54.52	O – 41.41 Si – 12.06 Zr – 46.53
Spectrum 2 Oxidized intermediate layer	O – 38.25 Si – 11.33 Zr – 47.81	O – 46.39 Si – 5.80 Zr – 36.77 B – 9.79 La – 0.55	O – 45.47 Si – 6.10 Zr – 46.96
Spectrum 3 Oxidized layer	O – 8.34 Si – 8.43 Zr – 48.42 B – 34.50	O – 24.96 Si – 3.45 Zr – 57.90 B – 13.13	O – 33.16 Si – 5.28 Zr – 53.60 B – 7.58

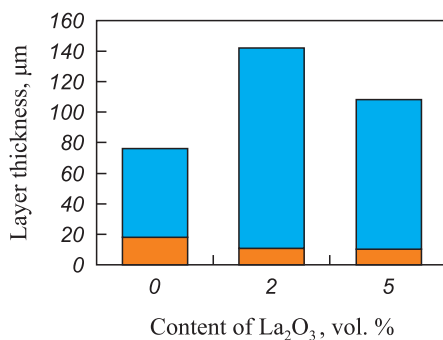


**Fig. 3.** Dependence of the thickness of oxidized layers on the surface of specimens of the  $\text{ZrB}_2$ -20 vol. %  $\text{SiC}$  composition without additives and with addition of 2 and 5 vol. %  $\text{La}_2\text{O}_3$  after oxidation for 20 h  
█ – spectrum 1, █ – spectrum 2 (see Fig. 2)  
The third layer is not shown because it was only partially in the imaging area

**Рис. 3.** Зависимость толщины окисленных слоев на поверхности образцов состава  $\text{ZrB}_2$ -20 об. %  $\text{SiC}$  без добавки и с введением 2 и 5 об. %  $\text{La}_2\text{O}_3$  после окисления в течение 20 ч  
█ – спектр 1, █ – спектр 2 (см. рис. 2)  
Третий слой не приведен, так как в зону съемки он попал лишь частично

Table 2 presents the results of calculating the atomic composition of the layers, with values rounded to the first decimal place after considering the atomic weights of the elements (and then multiplied by 10).

The assumed chemical composition is derived from the known composition of the initial specimens and the determined element ratios within the layers. The primary stoichiometric phases that are likely to be present are listed in Table 2. It should be noted that the formation of silicon monoxide as a crystalline compound has been previously documented in multiple instances [20–22].

The possibility of non-stoichiometric compound formation, such as borosilicate and borate glasses, should also be taken into consideration [23].

**Table 2. Ratio of elements in the layers after oxidation**

**Таблица 2. Соотношение элементов в слоях после окисления**

Imaging place (see Figure 2)	Ratio of elements and the most probable chemical composition with the $\text{La}_2\text{O}_3$ content, vol. %		
	0	2	5
Spectrum 1 Upper layer	$\text{Zr}_{0.3}\text{Si}_{19}\text{O}_{25}$ $\text{SiO}_2$ and $\text{SiO}$	$\text{Zr}_6\text{Si}_4\text{O}_{21}$ $\text{ZrSiO}_4$ and $\text{ZrO}_2$ Insignificant oxygen excess	$\text{Zr}_5\text{Si}_4\text{O}_{26}$ $\text{ZrSiO}_4$ and $\text{ZrO}_2$ Oxygen excess
Spectrum 2 Oxidized intermediate layer	$\text{Zr}_5\text{Si}_4\text{O}_{24}$ $\text{ZrSiO}_4$ and $\text{ZrO}_2$ Oxygen excess	$\text{Zr}_4\text{Si}_2\text{O}_{29}\text{B}_9$ $\text{ZrB}_2$ , $\text{ZrSiO}_4$ Oxygen excess	$\text{Zr}_5\text{Si}_2\text{O}_{28}$ $\text{ZrSiO}_4$ and $\text{ZrO}_2$ Oxygen excess
Spectrum 3 Oxidized layer	$\text{Zr}_5\text{Si}_3\text{O}_5\text{B}_{32}$ $\text{ZrB}_2$ , $\text{SiO}_2$ or $\text{SiO}$ Significant boron excess	$\text{Zr}_6\text{SiO}_{16}\text{B}_{12}$ $\text{ZrB}_2$ , $\text{SiO}_2$ Oxygen excess	$\text{Zr}_6\text{Si}_2\text{O}_{21}\text{B}_7$ $\text{ZrB}_2$ , $\text{ZrSiO}_4$ Oxygen excess

Raman spectroscopy confirmed the presence of zircon ( $\text{ZrSiO}_4$ ) and monoclinic zirconium dioxide ( $\text{ZrO}_2$ ) as the main phases of the oxidized material (Figure 4) [24]. The imaging was conducted from the surface of the specimens, thereby removing the first layer. One of the obtained spectra is presented, with the others being identical. The only distinction lies in the intensity ratio of the peaks corresponding to the main phases. The absence of silicon oxide lines in the specimen without lanthanum addition can be explained by the fact that well-oxidized phases in the second layer hinder the detection of amorphous or concealed-crystalline silicon oxide phases.

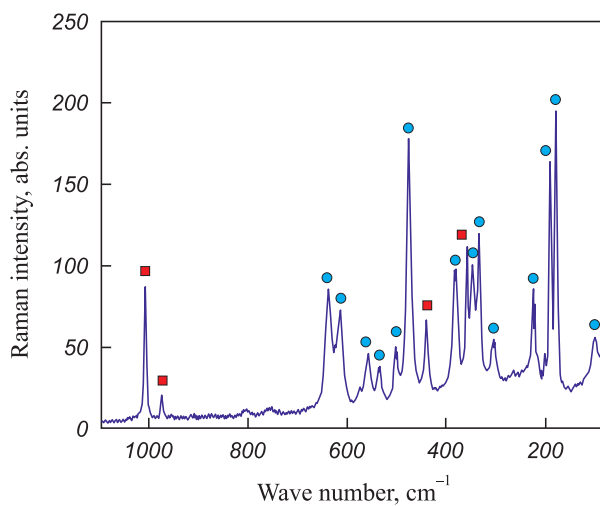


**Fig. 4.** Fragment of the Raman spectrum of the upper oxidized layer on the surface of a specimen with addition of 5 vol. %  $\text{La}_2\text{O}_3$  after oxidation for 20 h  
Designations of crystalline phases:  
█ – zircon; ● – monoclinic zirconium dioxide

**Рис. 4.** Фрагмент КР-спектра верхнего окисленного слоя на поверхности образца состава с добавкой 5 об. %  $\text{La}_2\text{O}_3$  после окисления в течение 20 ч  
Обозначения кристаллических фаз:  
█ – циркон; ● – моноклинный диоксид циркония

There is a noticeable disparity in the distribution of zirconium on the surface of specimens with and without  $La_2O_3$  (Figure 5, *a*–*c*). In the case without  $La_2O_3$ ,  $ZrO_2$ , despite its relatively low overall content (as seen in Table 1), is distributed relatively (Figure 5, *a*). Presumably, it is integrated within the primary silicon-containing phases. However, the addition of lanthanum oxide results in the growth of zirconium-bearing phase grains and the emergence of agglomerates and large pores between these phases. In this scenario, the formation of silicon oxides is unlikely.

Figure 5, *d* illustrates a fragment of the boron distribution map in the upper layer of the specimen containing 5 vol. %  $La_2O_3$ , corresponding to the fragment of the zirconium distribution map in Figure 5, *c*. Since boron could not be detected during the determination of the mass content of elements (as indicated in Table 1), it can be inferred that boron is present in the form of silicate glasses (refer to Figure 2, *f*) that fill the gaps between zircon and zirconium dioxide grains [25].

Consequently, on the surface of specimens without  $La_2O_3$  additives, phases comprising silicon oxides with traces of boron and zirconium oxides are formed. In the presence of  $La_2O_3$  additives, the main phases observed are zirconium dioxide and zircon, along with an excess of oxygen. However, neither case effectively acts as a significant barrier against the deep penetration of oxygen into the material. The presence of lanthanum oxide appears to enhance the formation of zircon, a phase that exhibits greater resistance to thermal shock than monoclinic zirconium dioxide and contributes to the deceleration of the oxidation process.

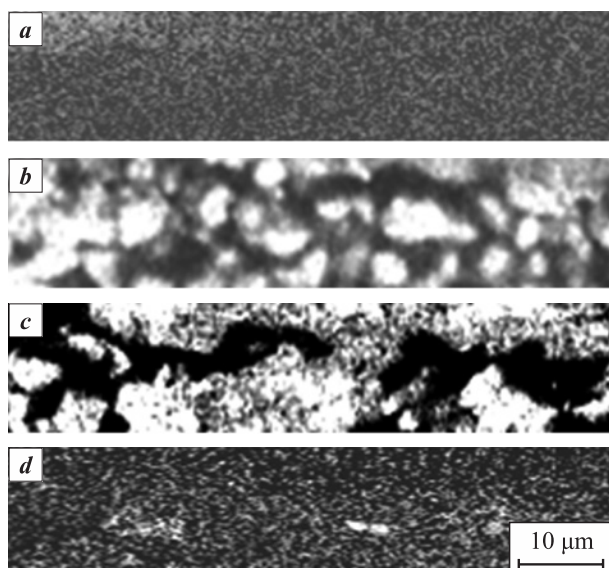


**Fig. 5.** Fragments of distribution maps of zirconium (*a*–*c*) and boron (*d*)

**Рис. 5.** Фрагменты карт распределения циркония (*a*–*c*) и бора (*d*)

## Conclusion

The aim of the study was to investigate the impact of  $La_2O_3$  addition on the oxidation properties of composite ceramics with a composition of 80 vol. %  $ZrB_2$  and 20 vol. %  $SiC$ , consolidated through spark plasma sintering. The materials were examined in three variations: without  $La_2O_3$ , with 2 vol. %  $La_2O_3$  and 5 vol. %  $La_2O_3$ . In all cases,  $SiC$  acted as a sacrificial material, being the first to undergo oxidation. Specimens without  $La_2O_3$  addition exhibited a surface layer consisting mainly of  $SiO_2$  and  $SiO$ . On the other hand, specimens with  $La_2O_3$  addition showcased surface layers composed primarily of  $ZrSiO_4$  and  $ZrO_2$ .

Consequently, the introduction of  $La_2O_3$  intensified the formation of zircon and decelerated the oxidation processes. However, it did not serve as a complete barrier to the deep penetration of oxygen into the material.

## References / Список литературы

1. Grigor'ev O.N., Frolov G.A., Evdokimenko Ju.I., Kisel' V.M., Panasjuk A.D., Melah L.M., Kotenko V.A., Koroteev A.V. Ultra-high temperature ceramics for aerospace technology. *Aviacionno-kosmicheskaja tekhnika i tehnologija*. 2012;8(95):119–128. (In Russ.).  
Григорьев О.Н., Фролов Г.А., Евдокименко Ю.И., Кисель В.М., Панасюк А.Д., Мелах Л.М., Котенко В.А., Коротеев А.В. Ультравысокотемпературная керамика для авиационно-космической техники. *Авиационно-космическая техника и технология*. 2012;8(95):119–128.
2. Naruckaja A.S., Istomin N.D. Oxidative behavior of high-temperature ceramics based on zirconium diboride. Prospects for the Development of Fundamental Sciences. In: *Proceedings of the XVIII International Conference of Students, Postgraduates and Young Scientists (Tomsk, 27–30.04.2021). Vol. 2. Khimija* (Eds. I.A. Kurzina, G.A. Voronova. Tomsk: Tomskii politehnicheskii universitet, 2021. P. 164–166. (In Russ.).  
Наруцкая А.С., Истомин Н.Д. Окислительное поведение высокотемпературных керамик на основе диборида циркония. Перспективы развития фундаментальных наук. В сб.: *Труды XVIII Международной конференции студентов, аспирантов и молодых ученых (Томск, 27–30 апреля 2021 г.). Т. 2. Химия*. Под ред. И.А. Курзиной, Г.А. Вороновой. Томск: Изд-во Томского политехнического университета, 2021. С. 164–166.
3. Iatsyuk I.V., Potanin A.Yu., Rupasov S.I., Levashov E.A. Kinetics and high-temperature oxidation mechanism of ceramic materials in  $ZrB_2$ – $SiC$ – $MoSi_2$  system. *Russian Journal of Non-Ferrous Metals*. 2018;59(1):76–81. <https://doi.org/10.3103/S1067821218010157>  
Яцюк И.В., Потанин А.Ю., Рупасов С.И., Левашов Е.А. Кинетика и механизм высокотемпературного окисления керамических материалов в системе  $ZrB_2$ – $SiC$ – $MoSi_2$ . *Известия вузов. Цветная металлургия*. 2017;(6): 63–69. <https://doi.org/10.17073/0021-3438-2017-6-63-69>

4. Zhitnyuk S.V. Oxygen-free ceramic materials for the space technologies (review). *Trudy VIAM*. 2018;(8):81–88. (In Russ.). <https://doi.org/10.18577/2307-6046-2018-0-8-81-88>  
Житнюк С.В. Бескислородные керамические материалы для аэрокосмической техники (обзор). *Труды ВИАМ*. 2018;(8):81–88.  
<https://doi.org/10.18577/2307-6046-2018-0-8-81-88>
5. Poilov V.Z., Pryamilova E.N. Thermodynamics of oxidation of zirconium and hafnium borides. *Russian Journal of Inorganic Chemistry*. 2016;61(1):55–58.  
<https://doi.org/10.1134/S0036023616010198>  
Пойлов В.З., Прямилова Е.Н. Термодинамика окисления боридов циркония и гафния. *Журнал неорганической химии*. 2016;61(1):59–62.  
<https://doi.org/10.7868/S0044457X16010190>
6. Li W., Cheng T., Li D., Fang D. Numerical simulation for thermal shock resistance of ultra high temperature ceramics considering the effects of initial stress field. *Advances in Materials Science and Engineering*. 2011;1–7:757543.  
<https://doi.org/10.1155/2011/757543>
7. Rangaray L., Surecha S.J., Divakar C., Jayaram V. Low-temperature processing of  $ZrB_2-ZrC$  composites by reactive hot pressing. *Metallurgical and Materials Transactions A*. 2008;39(7):1496–1505.  
<https://doi.org/10.1007/s11661-008-9500-y>
8. Gasch M.J., Ellerby D.T., Johnson S.M. Ultra high temperature ceramic composites. In: *Handbook of Ceramic Composites*. Boston: Springer, 2005. P. 197–224.  
[https://doi.org/10.1007/0-387-23986-3\\_9](https://doi.org/10.1007/0-387-23986-3_9)
9. Gozalez-Julian J., Cedillos-Barraza O., Döringet S. Enhanced oxidation resistance of  $ZrB_2/SiC$  composite through in situ reaction of gadolinium oxide in patterned surface cavities. *Journal of the European Ceramic Society*. 2014;34(16):4157–4166.  
<https://doi.org/10.1016/j.jeurceramsoc.2014.07.015>
10. Paul A., Jayaseelan D.D., Venugopal S., Zapata-Solvas E., Binner J., Vaidhyanathan B., Heaton A., Brown P., Lee W.E. UHTC composites for hypersonic applications. *American Ceramic Society Bulletin*. 2012; 91(1):22–29.
11. Chamberlain A., Fahrenholtz W., Hilmas G., Ellerby D. Oxidation of  $ZrB_2-SiC$  ceramics under atmospheric and reentry conditions. *Refractory Applications Transactions*. 2005;1(2):1–8.
12. Bellosi A., Monteverde F. Fabrication and properties of zirconium diboride-based ceramics for UHT applications. In: *Proc. 4<sup>th</sup> European Workshop. «Hot Structures and Thermal Protection Systems for Space Vehicles»* (Palermo, Italy 26–29 November 2002). Paris: European Space Agency, 2003. P. 65–71.
13. Justin J.F., Jankowiak A. Ultra high temperature ceramics: densification, properties and thermal stability. *AerospaceLab Journal*. 2011;3:1–11.
14. Bellosi A., Guicciardi S., Medri V., Monteverde F., Scitti D., Silvestroni L. Processing and properties of ultra-refractory composites based on Zr- and Hf-borides: state of the art and perspectives. In: *Boron rich solids: Sensors, ultra high temperature ceramics, thermoelectrics, armor*. 2011, P. 147–160. <https://doi.org/10.1007/978-90-481-9818-4>
15. Sonber J. K., Suri A. K. Synthesis and consolidation of zirconium diboride: review. *Advanced in applied ceramics. Structural, Functional and Bioceramics*. 2011;110(6):321–334. <https://doi.org/10.1179/174367611Y.0000000008>
16. Sciti D., Silvestroni L., Bellosi A. Fabrication and properties of  $HfB_2-MoSi_2$  composites produced by hot pressing and spark plasma sintering. *Journal of Materials Science*. 2006;21(6):1460–1466.  
<https://doi.org/10.1557/jmr.2006.0180>
17. Perevislov S.N., Nesmelov D.D., Tomkovich M.V.  $SiC$  and  $Si_3N_4$ -based materials obtained by spark plasma sintering. *Fizika tverdogo tela. Vestnik Nizhegorodskogo universiteta imeni N.I. Lobachevskogo*. 2013;2(2):107–114. (In Russ.).  
Перевислов С.Н., Несмелов Д.Д., Томкович М.В. Получение материалов на основе  $SiC$  и  $Si_3N_4$  методом высокотемпературного плазменного спекания. *Физика твердого тела. Вестник Нижегородского университета им. Н.И. Лобачевского*. 2013;2(2):107–114.
18. Hurbert D.M., Jiang D., Dudina D.V., Mukherjee A.K. The synthesis and consolidation of hard materials by spark plasma sintering. *International Journal of Refractory Metals and Hard Materials*. 2009;27(2):367–375.  
<https://doi.org/10.1016/j.ijrmhm.2008.09.011>
19. Hiller V.V. X-ray spectral microanalysis of boron content in the core of fiber blanks. problems of theoretical and experimental chemistry. In: *Abstracts of the XXIV Russian Youth Scientific Conference Dedicated to the 170<sup>th</sup> Anniversary of the Discovery of the Chemical Element Ruthenium* (Ekaterinburg, 23–25.04.2014). Yekaterinburg: Izdatel'stvo UrFU, 2014. P. 80–81. (In Russ.).  
Хиллер В.В. Рентгеноспектральный микроанализ содержания бора в сердцевине заготовок оптоволокна. Проблемы теоретической и экспериментальной химии. В сб.: *Тезисы докладов XXIV Российской молодежной научной конференции, посвященной 170-летию открытия химического элемента рутений* (Екатеринбург, 23–25 апреля 2014 г.). Екатеринбург: Издательство УрФУ, 2014. С. 80–81.
20. Gribov B.G., Zinov'ev K.V., Kalashnik O.N., Gerasimenko N.N., Smirnov D.I., Sukhanov V.N. Structure and phase composition of silicon monoxide. *Semiconductors*. 2012;46(13):1576–1579.  
<https://doi.org/10.1134/S106378261213009X>  
Грибов Б.Г., Зиновьев К.В., Калашник О.Н., Герасименко Н.Н., Смирнов Д.И., Суханов В.Н. Структура и фазовый состав монооксида кремния. *Известия вузов. Электроника*. 2011;4(90):3–8.
21. Al Kaabi Khalid, Prasad Dasari L.V.K., Kroll P. Silicon monoxide at 1 atm and elevated pressures: Crystalline or Amorphous? *Journal of the American Chemical Society*. 2014;136(9):3410–3423.  
<https://doi.org/10.1021/ja409692c>
22. Gribov B.G., Zinov'ev K.V., Kalashnik O.N., Gerasimenko N.N., Smirnov D.I., Sukhanov V.N. Growth of nanocrystalline silicon from a matrix of amorphous silicon monoxide. *Semiconductors*. 2013;47(13):1684–1686.  
<https://doi.org/10.1134/S1063782613130071>  
Грибов Б.Г., Зиновьев К.В., Калашник О.Н., Герасименко Н.Н., Смирнов Д.И., Суханов В.Н. Выращивание нанокристаллического кремния из матрицы аморфного монооксида кремния. *Известия вузов. Электроника*. 2012;96(4):13–18.

23. Ehrt D. Structure, properties and applications of borate glasses. *Glass Technology: European Journal of Glass Science and Technology. Part A*. 2000;41(6):182–185.
24. Orlov R.Yu., Vigasina M.F., Uspenskaya M.E. Raman spectra of minerals (reference book). Moscow: GEOS, 2007. 142 p. (In Russ.).  
Орлов Р.Ю., Вигасина М.Ф., Успенская М.Е. Спектры комбинационного рассеяния минералов: Справочник. М.: ГЕОС, 2007. 142 с.
25. Ban'kovskaya I.B., Kolovertnov D.V. Effect of the thermal treatment mode on the composition and structure of ZrB<sub>2</sub>–SiC system composites. *Glass Physics and Chemistry*. 2013;39(5):579–588.  
<https://doi.org/10.1134/S1087659613050027>  
Баньковская И.Б., Коловертнов Д.В. Влияние режима термообработки на состав и структуру композитов системы ZrB<sub>2</sub>–SiC. *Физика и химия стекла*. 2013;39(5):816–828.

**Information about the Authors**

**Valentina B. Kulmetyeva** – Cand. Sci. (Eng.), Associate Professor, Department of Mechanics of Composite Materials and Structures, Perm National Research Polytechnic University (PNRPU).

 **ORCID:** 0000-0002-5214-0932

 **E-mail:** kulmetevavb@pstu.ru

**Vyacheslav E. Chuvashov** – PhD student, Department of Mechanics of Composite Materials and Structures, PNRPU.

 **ORCID:** 0009-0000-0171-2024

 **E-mail:** slavachuvashov@yandex.ru

**Kseniya N. Lebedeva** – Master's Student, Department of Mechanics of Composite Materials and Structures, PNRPU.

 **ORCID:** 0009-0003-6134-2952

 **E-mail:** lebedkseni@mail.ru

**Svetlana E. Porozova** – Dr. Sci. (Eng.), Professor, Department of Mechanics of Composite Materials and Structures, PNRPU.

 **ORCID:** 0000-0001-5835-9727

 **E-mail:** sw.porozova@yandex.ru

**Maksim N. Kachenyuk** – Dr. Sci. (Eng.), Associate Professor, Department of Mechanics of Composite Materials and Structures, PNRPU.

 **ORCID:** 0000-0001-7476-9734

 **E-mail:** maxxkach@yandex.ru

**Сведения об авторах**

**Валентина Борисовна Кульметьева** – к.т.н., доцент кафедры механики композиционных материалов и конструкций (МКМК), Пермский национальный исследовательский политехнический университет (ПНИПУ).

 **ORCID:** 0000-0002-5214-0932

 **E-mail:** kulmetevavb@pstu.ru

**Вячеслав Эдуардович Чувашов** – аспирант кафедры МКМК, ПНИПУ.

 **ORCID:** 0009-0000-0171-2024

 **E-mail:** slavachuvashov@yandex.ru

**Ксения Николаевна Лебедева** – магистрант кафедры МКМК, ПНИПУ.

 **ORCID:** 0009-0003-6134-2952

 **E-mail:** lebedkseni@mail.ru

**Светлана Евгеньевна Порозова** – д.т.н., профессор кафедры МКМК, ПНИПУ.

 **ORCID:** 0000-0001-5835-9727

 **E-mail:** sw.porozova@yandex.ru

**Максим Николаевич Каченюк** – д.т.н., доцент кафедры МКМК, ПНИПУ

 **ORCID:** 0000-0001-7476-9734

 **E-mail:** maxxkach@yandex.ru

**Contribution of the Authors**

**V. B. Kulmetyeva** – conceptualization, goal setting, research objectives formulation, and thermal cycling of specimens.

**V. E. Chuvashov** – preparation of charge for spark plasma sintering, conducting high-temperature oxidation, data analysis, experimental results interpretation, of research result processing.

**K. N. Lebedeva** – analysis of experimental results, research results processing, article writing.

**S. E. Porozova** – scientific supervision, research results processing, text preparation and editing.

**M. N. Kachenyuk** – conducting spark plasma sintering.

**Вклад авторов**

**В. Б. Кульметьева** – постановка цели и задач исследования, формирование основной концепции, проведение термоциклирования образцов.

**В. Э. Чувашов** – подготовка шихты для проведения искрового плазменного спекания, подготовка и проведение высокотемпературного окисления, проведение расчетов, анализ полученных результатов экспериментов, обработка результатов исследований.

**К. Н. Лебедева** – анализ полученных результатов экспериментов, обработка результатов исследований, подготовка текста статьи.

**С. Е. Порозова** – научное руководство, обработка результатов исследований, подготовка и корректировка текста статьи.

**М. Н. Каченюк** – проведение искрового плазменного спекания.

Received 22.06.2022

Revised 11.11.2022

Accepted 19.12.2022

Статья поступила 22.06.2022 г.

Доработана 11.11.2022 г.

Принята к публикации 19.12.2022 г.